

m6A and NuRD complexes regulate monocytic differentiation and resistance to BCL2/BCL2L1 inhibitors in acute myeloid leukemia

Jackson Brim-Edwards,^{1,2} Karen Morris,^{1,2} Quinlan Morrow,^{1,2} Stephen E. Kurtz,^{2,3} Daniel Bottomly,² Shannon K. McWeeney,^{2,4} Cristina E. Tognon,^{2,3} Tamilla Nechiporuk,^{1,2} Kevin Watanabe-Smith^{2,3#} and Jeffrey W. Tyner^{1,2,5#}

¹Department of Cell, Developmental & Cancer Biology; ²Knight Cancer Institute; ³Division of Oncological Sciences, Knight Cancer Institute; ⁴Division of Bioinformatics and Computational Biology, Department of Medical Informatics and Clinical Epidemiology and ⁵Division of Hematology and Medical Oncology, Oregon Health & Science University, Portland, OR, USA

[#]KW-S and JWT contributed equally as senior authors.

Correspondence: J.W. Tyner
tynerj@ohsu.edu

Received: April 9, 2025.

Accepted: October 3, 2025.

Early view: October 16, 2025.

<https://doi.org/10.3324/haematol.2025.287972>

©2026 Ferrata Storti Foundation

Published under a CC BY-NC license



Abstract

Frontline use of the BCL2 inhibitor, venetoclax, for acute myeloid leukemia (AML) has resulted in broad improvements in patients' outcomes. A major remaining challenge is the development of venetoclax resistance, frequently driven by compensatory transcriptional programs that promote cell survival and differentiation. These changes reduce dependence on BCL2 in favor of alternative anti-apoptotic BCL2 family members such as MCL1 or BCL2L1 (BCL-X_L). Using CRISPR-based genome-wide perturbation screens, we investigated the genetic dependencies of venetoclax and the BCL2/BCL2L1 dual inhibitor AZD4320. We identified the N6-methyladenosine (m6A) writer RBM15, and the nucleosome remodeling and deacetylase (NuRD) complex interactor ZMYND8 as novel mediators of resistance to both venetoclax and AZD4320. Loss of *RBM15* or *ZMYND8* induced drug resistance, concurrent with alterations in BCL2 family expression and monocytic differentiation. Accordingly, in AML patients' samples we found reduced expression of the respective m6A or NuRD complexes was significantly associated with monocytic differentiation and *ex vivo* resistance to the same drugs. These findings provide critical insights into previously undescribed mechanisms of BCL2 family inhibitor resistance in AML.

Introduction

The BCL2 family of apoptosis regulators has emerged as a promising therapeutic target in acute myeloid leukemia (AML).¹ This family includes anti-apoptotic proteins such as BCL2, MCL1, and BCL2L1 (BCL-X_L), which block apoptosis by binding and neutralizing pro-apoptotic effectors BAX and BAK – proteins essential for mitochondrial outer membrane permeabilization.² Venetoclax, a BH3 mimetic that selectively binds and inhibits BCL2, has demonstrated significant efficacy in AML and is approved by the Food and Drug Administration for use in combination with hypomethylating agents to improve response rates and overall survival.³⁻⁶

Prior CRISPR-based genome-wide perturbation screens have identified key genes and pathways that mediate the response to venetoclax. Downregulation of pro-apoptotic

effectors – BAX, PMAIP1 (NOXA), and TP53 – or compensatory upregulation of MCL1 and BCL2L1, results in venetoclax-resistance in AML cells.^{5,7,8} Cellular differentiation state has also been implicated in resistance, with more differentiated monocytic or megakaryocytic/erythroid cells displaying increased resistance to venetoclax, often accompanied by upregulation of MCL1, BCL2L1, or BCL2A1 relative to BCL2.⁸⁻¹⁸ These findings underscore the importance of addressing both changes in the baseline expression of BCL2 proteins and the upregulation following treatment, such as treatment-induced resistance. To address one avenue of resistance, BCL2L1 (BCL-X_L) overexpression, dual inhibitors targeting both BCL2 and BCL2L1 – including AZD4320 and navitoclax – have been developed.^{19,20} To identify both shared and unique mechanisms of resistance between AZD4320 and those previously identified for venetoclax, we performed

a genome-wide CRISPR/Cas9 screen in OCI-AML2 cells cultured with AZD4320. Here, we identified RBM15 and ZMYND8 as novel key dependencies for the response to both venetoclax and AZD4320.

RBM15 is a component of the m6A RNA methylation machinery, the most common internal mRNA modification, which regulates transcript splicing, export, stability, translation, and degradation. The core m6A “writer” methyltransferase complex includes METTL3, METTL14, and WTAP, with RBM15 acting as an adaptor to recruit the complex to specific RNA sites. m6A “reader” proteins, such as YTHDF family members, mediate the effects of m6A on RNA metabolism, while “erasers”, like FTO and ALKBH5, reverse the modification, dynamically regulating transcript expression.^{21,22} In leukemia, the t(1;22)(p13;q13) translocation results in a *RBM15-MKL1* (OTT-MAL) fusion gene, which is linked to a rare subtype of acute megakaryoblastic leukemia in infants.²³

ZMYND8, a multifunctional epigenetic regulator within the NuRD complex, modulates chromatin structure and transcriptional repression. The NuRD complex, composed of histone deacetylases (HDAC1/2), chromatin remodeling ATPases (CHD3/4), and metastasis-associated proteins (MTA1-3), facilitates chromatin compaction and gene silencing.^{24,25} ZMYND8 mediates NuRD complex targeting to specific histone modifications including H3K36me2/3 and H4K16Ac. Recent studies have identified NuRD²⁶ and ZMYND8^{27,28} as essential for AML cell survival by regulating transcriptional programs crucial for leukemogenesis.

In AML, dysregulation of m6A methylation has been implicated in leukemogenesis by modulating the expression of genes involved in self-renewal and differentiation of hematopoietic stem and progenitor cells.^{29,30} Similarly, dysregulated NuRD activity alters the expression of genes critical for myeloid maturation, thereby maintaining leukemic cells in an undifferentiated state.³¹

Methods

Cell lines and culture conditions

OCI-AML2 human AML cell lines were obtained from the American Type Culture Collection. Cells were cultured in RPMI-1640 medium supplemented with 20% fetal bovine serum, L-glutamine, penicillin-streptomycin, and amphotericin B. Cultures were maintained at 37°C with 5% CO₂ and were routinely tested for *Mycoplasma* contamination.

Genome-wide CRISPR/Cas9 screening

Loss-of-function screens were performed using the Y. Kosuke³² human genome-wide sgRNA library. Cells were treated with 30 nM AZD4320 or dimethylsulfoxide (DMSO) control for 14 days. Genomic DNA was extracted, and sgRNA sequences were amplified for Illumina sequencing. Reads were trimmed using cutadapt (v2.3)³³ to extract the candidate sequences. Alignment was then performed using

Bowtie2 (v2.3.5.1)³⁴ relative to a custom set of expected sgRNA sequences. After conversion to Bam format, unique matches were selected using Bamtools (v2.5.1).³⁵ Reads were counted for each sample using MAGeCK. The counts were next filtered for low representation (those not in the plasmid-only samples or those with ≤100 counts per million in more than half the samples) and then normalized using the trimmed mean of M. The edgeR package³⁶ was used for each linear model, generating log₂ fold changes and two-sided *P* values. Gene-level tiering was performed as described previously.⁷

Generation and validation of knockout cell lines

RBM15 and *ZMYND8* knockout (KO) cell lines were generated by transducing OCI-AML2 cells with sgRNA-containing lentiviral particles. Two biologically distinct lines were generated for each condition using separate sgRNA sequences. Puromycin selection was applied for 7 days. Knockout efficiency was validated via western blotting.

Cell proliferation assays

Wild-type, non-targeting control, *RBM15* KO and *ZMYND8* KO OCI-AML2 cells were cultured for 6 days in 30 nM AZD4320 or DMSO. Viable cells were counted every 2 days to assess proliferation.

RNA sequencing and analysis

Total RNA was extracted from wild-type, non-targeting control, *RBM15* knockout, and *ZMYND8* knockout cells. Stranded poly(A)⁺ RNA sequencing libraries were prepared and sequenced in triplicate on an Illumina NovaSeq 6000 platform, generating 150 bp paired end reads. Reads were trimmed using Trimmomatic and aligned to the human reference genome (GRCh38/hg38) using STAR aligner. Differential expression analysis was performed using DESeq2, with surrogate variable analysis applied for batch effect correction. Genes with an adjusted *P* value <0.05 and an absolute log₂ fold change >1 were considered differentially expressed. Cell type enrichment was analyzed using the Panglao DB database in R.

BCL2 family gene ratios were calculated as a ratio of normalized counts using DESeq2's median of ratios normalization. Statistical significance was calculated using a two-sided Student *t* test comparing the six values from the non-targeted lines (2 biological lines, 3 replicates each) to the six values of the indicated knockout line.

Human subject data and ethical approval

The patients' data used in this study were obtained from the publicly available Beat AML dataset, which includes de-identified clinical data. Use of this dataset was approved by the Oregon Health & Science University Institutional Review Board (OHSU IRB). All protocols involving human subjects' data were conducted in accordance with the ethical standards of the OHSU IRB.

Results

Genome-wide CRISPR screen revealed novel transcriptional regulators controlling BCL2 inhibitor resistance

While acquired resistance to venetoclax supports the development of dual BCL2/BCL2L1 inhibitors (Figure 1A), it is unknown whether unique predictors of drug response exist for BCL2-selective inhibitors versus BCL2/BCL2L1 inhibitors. To address this question, we first analyzed data from *ex vivo* screening of primary AML samples. This approach demonstrated a robust relationship between responses to venetoclax and AZD4320 for individual patients' samples

(Figure 1B). By integrating *ex vivo* AZD4320 screening of 232 primary AML samples with the existing Beat AML transcriptomic dataset, we directly compared the correlations between gene expression and drug response in a shared set of samples. While slight outliers were observed, the correlations between gene expression and area under the curve for venetoclax were largely similar in both direction and magnitude to those observed for AZD4320 (Figure 1C). To investigate global resistance mechanisms for AZD4320, we conducted a genome-wide CRISPR screen in OCI-AML2 cells treated with 30 nM AZD4320 for 14 days (Figure 2A). We identified several shared, evidence-based tiered hits between both AZD4320 and venetoclax⁷ screens, including

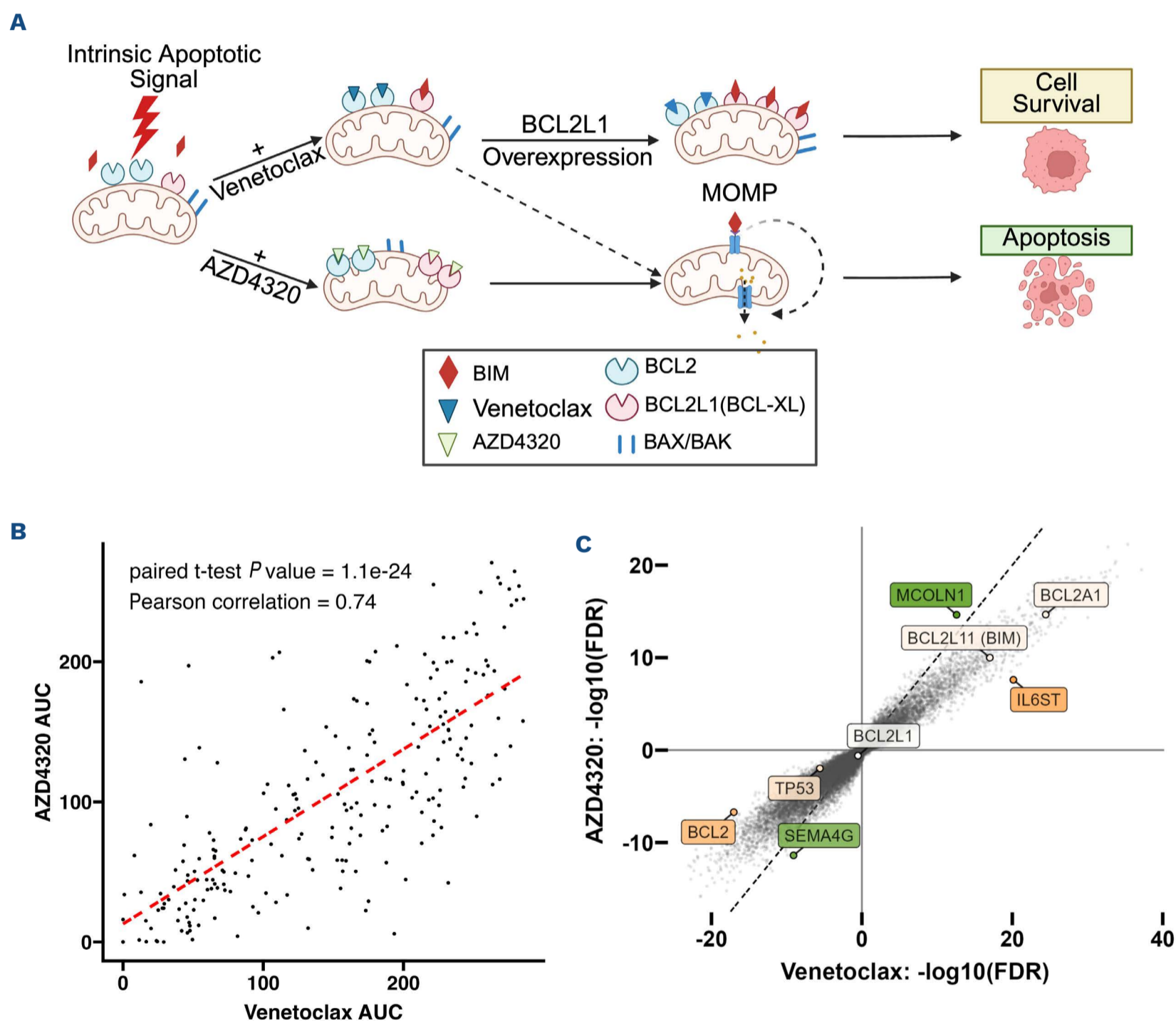


Figure 1. AZD4320 overcomes BCL2L1-mediated resistance and mirrors venetoclax sensitivity in acute myeloid leukemia. (A) Schematic of the differential action of venetoclax and AZD4320. Upregulation of BCL2L1 (BCL-X_L) confers resistance to venetoclax but not to AZD4320. (B) Comparison of area under the curve values between venetoclax and AZD4320 for 232 AML patients' samples from the BEAT AML database. (C) Pearson correlation of gene expression and *ex vivo* drug response to venetoclax (x-axis) and AZD4320 (y-axis). Signed, log-transformed false discovery rate-corrected P values are shown for venetoclax (x-axis) and AZD4320 (y-axis). The dotted line indicates the $x=y$ line; select BCL2-family genes and outliers are labeled. MOMP: mitochondrial outer membrane permeabilization; AUC: area under the curve; FDR: false discovery rate.

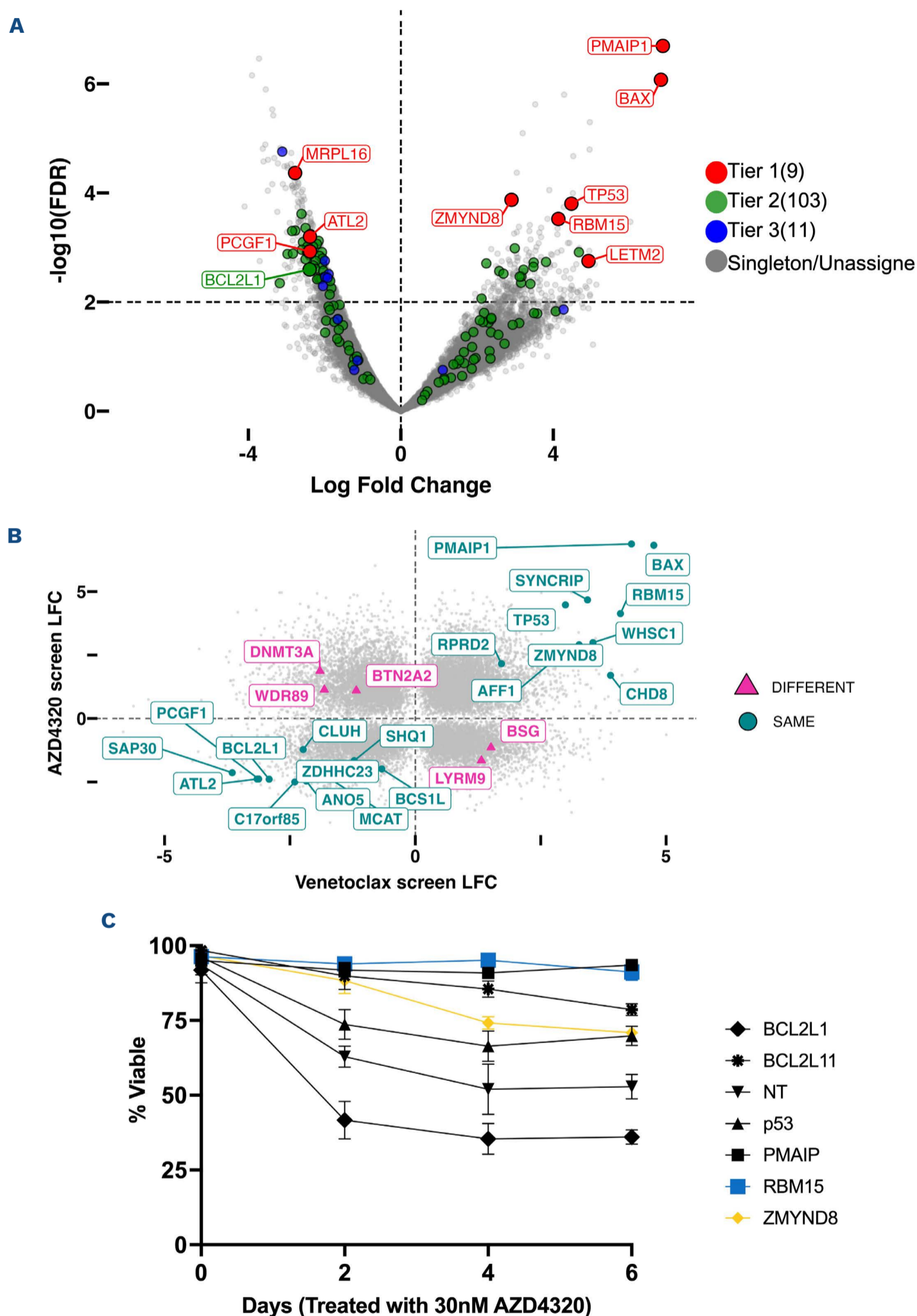


Figure 2. Genome-wide CRISPR screens identify *RBM15* and *ZMYND8* as AZD4320 resistance hits. (A) CRISPR screen results display log-fold changes and significance of changes in sgRNA abundance in OCI-AML2 cells over 14 days of AZD4320 (30 nM) treatment when compared to those in dimethylsulfoxide-treated controls. Genes are stratified into confidence tiers based on effect size and concordance between multiple guides. (B) Comparison of AZD4320 and venetoclax CRISPR screens on OCI-AML2 cells; genes that were classified as tier 1, 2, or 3 hits in both screens are labeled, including discordant genes (in maroon). (C) Viability of OCI-AML2 cells with single-gene knockouts (KO) while cultured in 30 nM AZD4320; *RBM15*-KO and *ZMYND8*-KO are highlighted in blue and yellow respectively. NT: non-targeting; LFC: log-fold change.

drug-resistance following loss of *PMAIP1*, *BAX* and *TP53*, and increased sensitivity following loss of *BCL2L1* (Figure 2B). Relatively few genes produced discordant hits between the screens, and while promising for future study, the smaller effect sizes in this group led us to prioritize investigation of the strongest shared hits.

Notably, we identified two novel tier 1 hits, *RBM15* and *ZMYND8*, as regulators of drug response in both the AZD4320 and venetoclax screens.^{7,15} To validate these findings, we generated *RBM15* and *ZMYND8* KO OCI-AML2 cell lines using lentiviral CRISPR-Cas9 gene editing, with successful knock-out confirmed via western blotting (*Online Supplementary Figure S1A*). These cells displayed significantly increased resistance (one-way analysis of variance with the Dunnett test: *RBM15* $P=0.0001$; *ZMYND8* $P=0.0075$) to AZD4320 compared to non-targeting cells in outgrowth assays (Figure 2C, *Online Supplementary Figure S1B*) and dose-response analyses (*Online Supplementary Figure S1C, D*) compared to non-targeting controls. Notably, response to non-BCL2-directed inhibitors (including trametinib, midostaurin, and sorafenib) were not similarly affected by loss of *RBM15* or *ZMYND8* (*Online Supplementary Figure S1E*).

***RBM15* and *ZMYND8* knockout drives changes in BCL2 expression and differentiation consistent with primary acute myeloid leukemia samples**

To examine the mechanisms by which loss of *RBM15* or *ZMYND8* confers resistance to BCL2 inhibitors, we first performed RNA-sequencing on OCI-AML2 knockout cell lines, followed by gene set enrichment analysis (GSEA) to identify pathways previously implicated in venetoclax resistance (*Online Supplementary Figure S2A, B*). There appeared to be little upregulation of the pathways commonly associated with drug resistance to BCL2 inhibitors such as *MAPK/ERK* and *TP53* pathways.

The relative ratios of BCL2 family member expression are highly predictive of *in vitro* and clinical response to venetoclax, such that cells with lower ratios of *BCL2* relative to *BCL2L1* or *MCL1* are resistant to venetoclax.³⁷⁻³⁹ Accordingly, we next examined relative RNA expression of BCL2 family members following the knockout of *RBM15* or *ZMYND8*. In *ZMYND8* KO cell lines we did indeed detect a reduction in the ratio of *BCL2* to *MCL1* ($P=0.001$, $t=4.73$) and *BCL2* to *BCL2L1* ($P<0.0001$, $t=9.72$), suggesting an increased reliance on these *BCL2* alternatives for evading drug-induced apoptosis (Figure 3A). Interestingly, in *RBM15* KO cell lines, we did not detect changes in any of the pro-survival members of the BCL2 family, but instead we observed elevated ratios of *BCL2L1* to *BCL2L11* (*BIM*) ($P=0.002$, $t=-4.51$) and *BCL2* to *BIM* ($P=0.0006$, $t=-5.06$), suggesting a novel mechanism of resistance whereby the increased proportion of pro-survival BCL2 family members relative to the apoptotic initiator BIM may shift the balance toward survival, reducing apoptotic priming and limiting drug efficacy.

We next explored whether these changes in BCL2 family

expression in the setting of *RBM15*- and *ZMYND8*-loss are linked to altered AML cell maturation state and assessed whether knockout of these genes influenced differentiation. GSEA of upregulated genes in knockout cell lines, using PanglaoDB-derived cell type annotations,⁴⁰ revealed enrichment of differentiated myeloid cell states in both *RBM15*- and *ZMYND8*-KO lines (Figure 3B). These included macrophage-like (normalized enrichment score [NES]=2.28, false discovery rate [FDR]= 1.80×10^{-7}), monocytic-like (NES=2.17, FDR= 4.29×10^{-5}), and dendritic-like cell types (NES=2.21, FDR= 1.12×10^{-5}).

To further investigate the relationship between *RBM15* and *ZMYND8* expression and differentiation, we evaluated their association with clinical differentiation markers in primary AML samples. Using linear regression, we found that lower expression of both genes was significantly associated with increased percentages of peripheral blood monocytes (*RBM15*: $t=-5.45$, $P<9.19\times 10^{-8}$; *ZMYND8*: $t=-2.92$, $P<0.003$), consistent with a more differentiated phenotype (Figure 4A). Next, expression of these genes was compared to expression-derived AML-specific cell state scores.⁴¹ Spearman correlation analysis revealed that *RBM15* and *ZMYND8* expression levels were positively associated with more primitive states, including progenitor-like (*ZMYND8*: $\rho=0.18$, FDR $<3.14\times 10^{-5}$; *RBM15*: $\rho=0.16$, FDR $<1.8\times 10^{-4}$) and hematopoietic stem cell-like states (*ZMYND8*: $\rho=0.17$, FDR $<8.2\times 10^{-5}$; *RBM15*: $\rho=0.23$, FDR $<1.62\times 10^{-5}$). Conversely, both genes were negatively correlated with more differentiated states such as promonocytic-like (*ZMYND8*: $\rho=-0.23$, FDR $<2.14\times 10^{-7}$; *RBM15*: $\rho=-0.11$, FDR $<1.18\times 10^{-2}$) and monocyte-like phenotypes (*ZMYND8*: $\rho=-0.17$, FDR $<7.77\times 10^{-5}$; *RBM15*: $\rho=-0.10$, FDR $<1.35\times 10^{-5}$) (Figure 4A, *Online Supplementary Figure S3B, C, E, F*).

Given that differentiation status is a known predictor of venetoclax sensitivity,^{8-10,12} we wanted to see whether a similar effect would be observed with AZD4320. Using Spearman correlation, we found a positive association between peripheral blood monocyte percentages from primary AML samples and AZD4320 response ($\rho=0.51$, $P<1.12\times 10^{-5}$), consistent with previously reported venetoclax sensitivity patterns (Figure 4B, *Online Supplementary Figure S3A, D*).

In contrast to cell line models, in which gene expression and drug response were strongly linked, we found that Spearman correlations between *ex vivo* venetoclax or AZD4320 response and *RBM15* or *ZMYND8* expression in primary samples were weak or non-significant (venetoclax: *RBM15*: $\rho=-0.009$, FDR=0.85; *ZMYND8*: $\rho=-0.14$, FDR <0.004 ; AZD4320: *RBM15*: $\rho=-0.11$, FDR=0.094; *ZMYND8*: $\rho=-0.15$, FDR <0.02) (Figure 4C). Abundance of *ZMYND8* protein showed a modest but stronger inverse correlation with drug response, while *RBM15* protein expression remained non-significant (*Online Supplementary Figure S2C-F*).

Expanded analysis of m6A RNA methylation and NuRD chromatin remodeling complexes

Given that *RBM15* and *ZMYND8* expression as individual

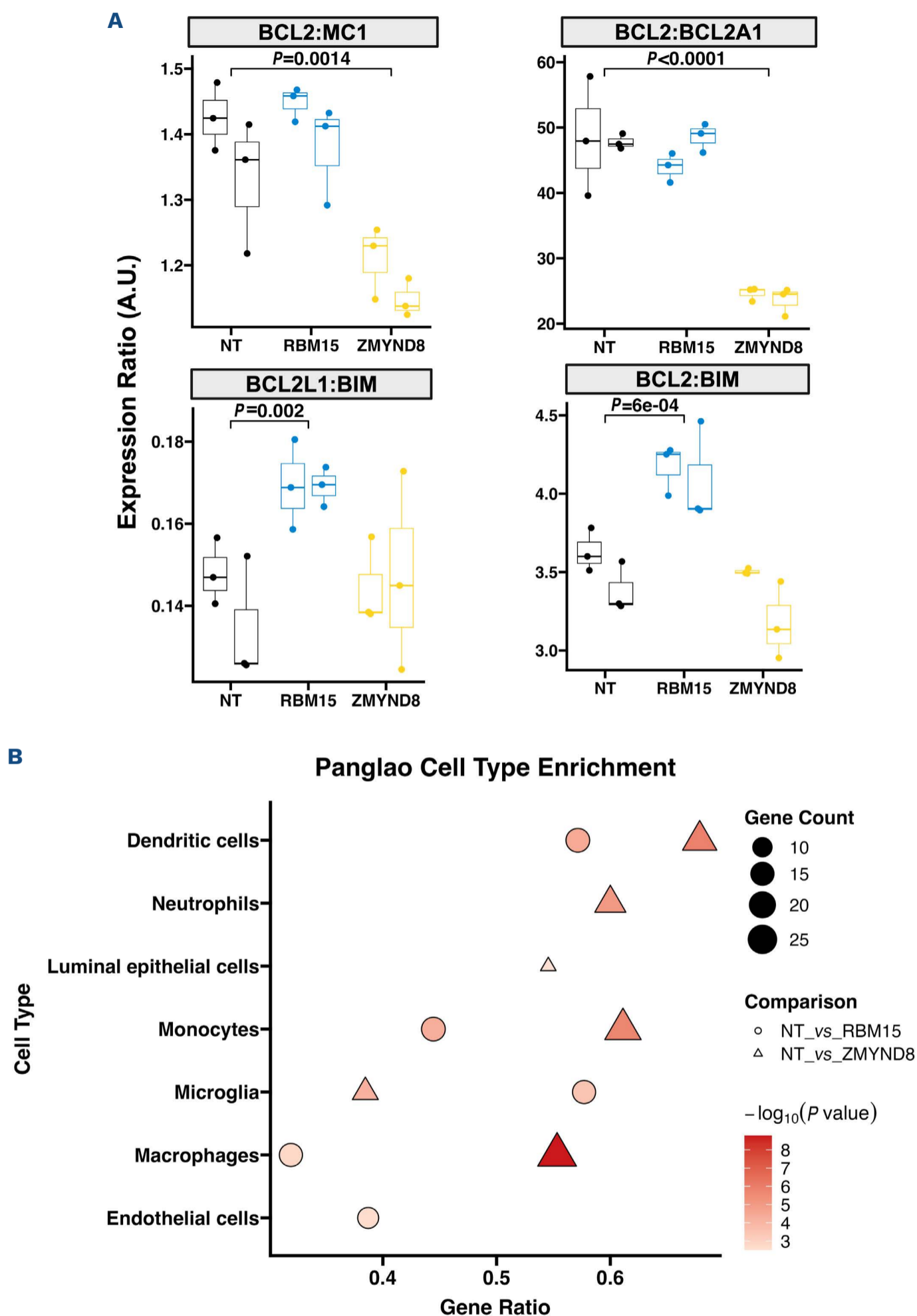


Figure 3. *RBM15* and *ZMYND8* knockout alters apoptotic balance and promotes myeloid differentiation. (A) Ratios of BCL2 family member expression in OCI-AML2 cells following single-gene knockout (KO). Biological replicates generated with distinct sgRNA are shown for each knockout, and three technical replicates for each line. *ZMYND8* KO cells show significant reduction in BCL2 relative to other anti-apoptotic members, MCL1 and BCL2A1 (two-sided *t* test *P* value shown). *RBM15* KO cells show significantly increased expression of AZD4320 targets BCL2L1 and BCL2 relative to the apoptotic initiator BCL2L1 (BIM). (B) Gene set enrichment analysis of differentially expressed genes between *RBM15* KO and *ZMYND8* KO lines against non-targeted control lines shows increased enrichment of differentiated myeloid cell states – including neutrophil-like, macrophage-like, and monocyte-like – in both knockout lines, with odds ratios and false discovery rate-adjusted *P* values indicating statistical significance. A.U.: arbitrary units; NT: non-targeted.

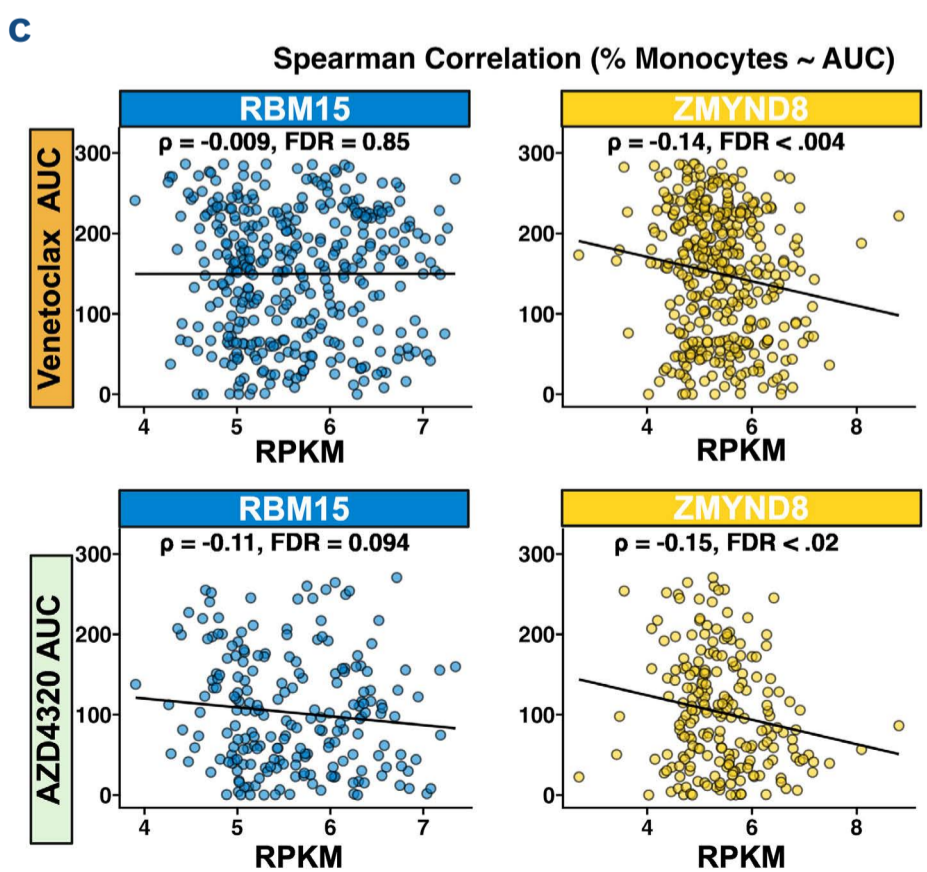
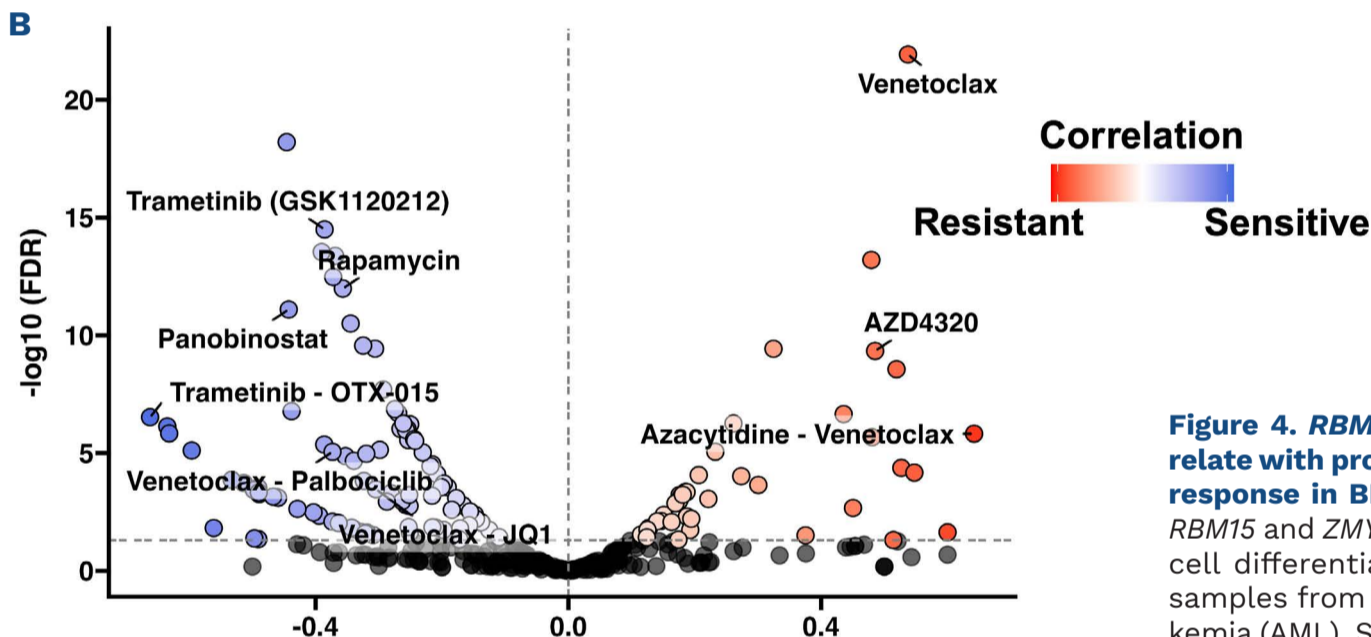
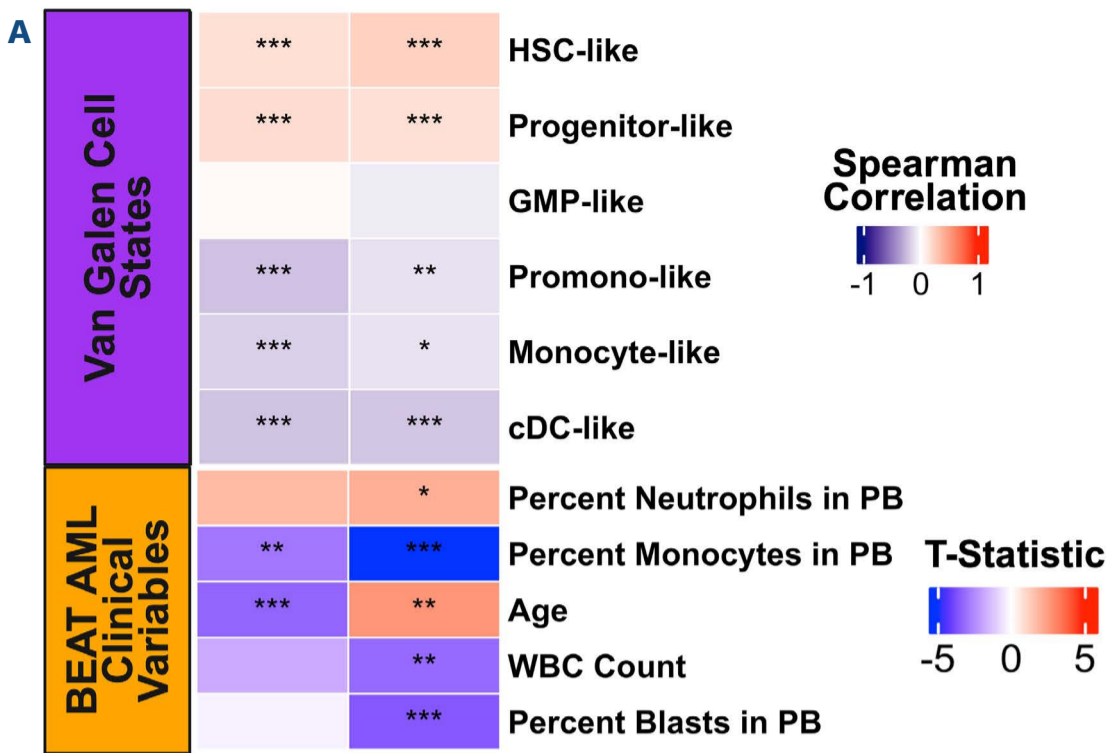


Figure 4. *RBM15* and *ZMYND8* expression correlate with progenitor states and *BCL2* inhibitor response in BEAT AML data. (A) Correlation of *RBM15* and *ZMYND8* expression with RNA-derived cell differentiation states and clinical data in samples from patients with acute myeloid leukemia (AML). Spearman correlation was used for associations with inferred differentiation states, while linear regression was used for clinical variables. Both genes show higher expression in progenitor-like states and lower expression in more differentiated cell types. The *t* statistic reported is derived from our linear regression. Additionally, strong negative correlations were observed between gene expression and monocyte abundance in peripheral blood. ($*P < 0.05$, $**P < 0.01$, $***P < 0.001$). (B) Association of monocyte abundance in patients' samples with drug response (AUC) to venetoclax, AZD4320, and other inhibitors. Both AZD4320- and venetoclax-responses are highly correlated with monocyte abundance. (C) Scatter plots of *RBM15* and *ZMYND8* expression versus *ex vivo* drug response for venetoclax and AZD4320 in primary AML samples, showing no significant Spearman correlation for *RBM15* expression and a moderate correlation for *ZMYND8* expression with drug sensitivity. HSC: hematopoietic stem cells; cDC: classical dendritic cell; PB: peripheral blood; WBC: white blood cell; FDR: false discovery rate; AUC: area under the curve; RPKM: reads per kilobase million.

genes did not correlate strongly with drug response in patients' samples, we expanded our analysis to include the broader m6A RNA methylation and NuRD chromatin remodeling complexes, in which RBM15 and ZMYND8 serve as key components. Using either RNA-sequencing (*Online Supplementary Figure S4A*) or whole-proteome quantification (liquid chromatography and tandem mass spectrometry) of patients' samples (Figures 5A and 6A), we performed principal component analysis (PCA) to generate eigengene-like signatures for each complex (*Online Supplementary Table S1*), capturing overall pathway activity through unsupervised composite profiles.

Principal component analysis of m6A and NuRD complexes

To assess m6A pathway activity, we performed PCA on protein abundance data for core m6A complex members, generating an eigengene-like representation of pathway activity (m6A PC1) (Figure 5A). Most proteins loaded positively onto PC1, supporting its interpretation as a proxy of overall m6A complex activity. Linear regression analysis revealed that m6A PC1 was negatively associated with peripheral blood monocyte percentage ($t = -2.25$, $FDR < 0.03$) and positively associated with peripheral blood blast percentage⁴² ($t = 7.89$, $FDR < 1 \times 10^{-11}$), suggesting that reduced m6A pathway activity corresponds to more differentiated cell states (Figure 5B). Similarly, PCA of NuRD complex protein abundance generated a NuRD eigengene-like signature (NuRD PC1), representing overall pathway activity (Figure 6A). Most pathway components loaded positively onto PC1, analogous to the m6A analysis. Using linear regression, we found that NuRD PC1 was negatively associated with peripheral blood monocyte percentage ($t = -3.64$, $FDR < 7.55 \times 10^{-4}$) and positively associated with peripheral blood blast percentage ($t = 5.54$, $FDR < 7.1 \times 10^{-7}$), supporting the interpretation that reduced NuRD complex activity corresponds to a more differentiated disease state. Both of these pathway principal components correlated with expression-derived AML cell state scores,⁴¹ which reinforced these findings. Spearman correlation analysis demonstrated that the m6A PC1 was strongly negatively correlated with monocyte-like states ($\rho = -0.68$, $FDR < 1.04 \times 10^{-17}$) and positively correlated with primitive states, including progenitor-like ($\rho = 0.70$, $FDR < 2.55 \times 10^{-19}$) and hematopoietic stem cell-like states ($\rho = 0.28$, $FDR < 1.03 \times 10^{-3}$) (Figure 5B). Similarly, NuRD PC1 was negatively correlated with monocyte-like states ($\rho = -0.59$, $FDR < 5.6 \times 10^{-13}$) and positively correlated with progenitor-like ($\rho = 0.62$, $FDR < 1.1 \times 10^{-14}$) and hematopoietic stem cell-like states ($\rho = 0.44$, $FDR < 3.2 \times 10^{-7}$) (Figure 6B). These data collectively support a model in which reduced m6A and NuRD complex activities are linked to more differentiated AML cell states, consistent with their proposed roles in maintaining cellular primitiveness.

Drug sensitivity analysis

To explore the potential therapeutic impact of these path-

ways, we assessed the correlation between each principal component and *ex vivo* response to several small molecule inhibitors in primary AML samples. Both the m6A and NuRD PC1 were negatively correlated with sensitivity to AZD4320 (m6A: $\rho = -0.49$, $FDR < 3.7 \times 10^{-4}$; NuRD: $\rho = -0.48$, $FDR < 6.72 \times 10^{-4}$) and venetoclax (m6A: $\rho = -0.49$, $FDR < 5.3 \times 10^{-6}$; NuRD: $\rho = -0.49$, $FDR < 6.9 \times 10^{-6}$) (Figures 5C and 6C). These findings suggest that reduced m6A and NuRD pathway activity is associated with resistance to BCL2 inhibitors, consistent with prior observations that differentiated AML subtypes are less sensitive to these therapies. This setting of reduced expression of m6A or NuRD pathways correlates with sensitivity to certain drugs, including inhibitors of histone deacetylases (panobinostat), MTOR (rapamycin), and a kinase inhibitor (nilotinib). Similar analyses using RNA data to generate expression-derived principal component scores yielded comparable results for both pathways (*Online Supplementary Figure S4A-F*).

Overall, these findings highlight the strong link between m6A and NuRD pathway activities and AML differentiation, demonstrating that reduced pathway activity or disruption contributes to decreased sensitivity to BCL2 inhibitors in a differentiation-dependent manner.

Discussion

Venetoclax, a selective BCL2 inhibitor, has significantly advanced the treatment of AML, particularly in older patients unfit for intensive chemotherapy, when used in combination with hypomethylating agents. However, despite promising initial responses, resistance to venetoclax remains a major clinical hurdle, leading to relapse in many patients. Here, we identify *RBM15* and *ZMYND8* as novel mediators of resistance to both venetoclax and the dual BCL2/BCL2L1 inhibitor AZD4320 in the OCI-AML2 cell line. Notably, the loss of either gene induces differentiation toward a monocytic phenotype, resulting in resistance to BCL2 inhibition. This observation aligns with previous findings that more differentiated AML cells exhibit inherent resistance to venetoclax.⁸⁻¹⁸

Using genome-wide CRISPR screens, we confirmed that apoptotic regulators known to control the response to venetoclax, such as *BAX*, *PMAIP1*, and *TP53*,⁷ are similarly involved in the response to AZD4320. While highly similar drugs, primary samples indicate that expression of a few genes, including *BCL2*, *TP53BP1*, and *IL6ST*, are more correlated to venetoclax response. Genes more predictive of AZD4320 response include *MCOLN1* (which inhibits apoptosis in a BAX-dependent manner) and *SEMA4G*.⁴³ Notably *SEMA4G* is not linked to the BCL2 family, but the intron of *SEMA4G* contains *miR-608*, which promotes apoptosis in prostate cancer cells by inhibiting *BCL2L1* translation through directly binding the 5' untranslated region.⁴⁴ We were unable to detect expression of the short *miR-608* in

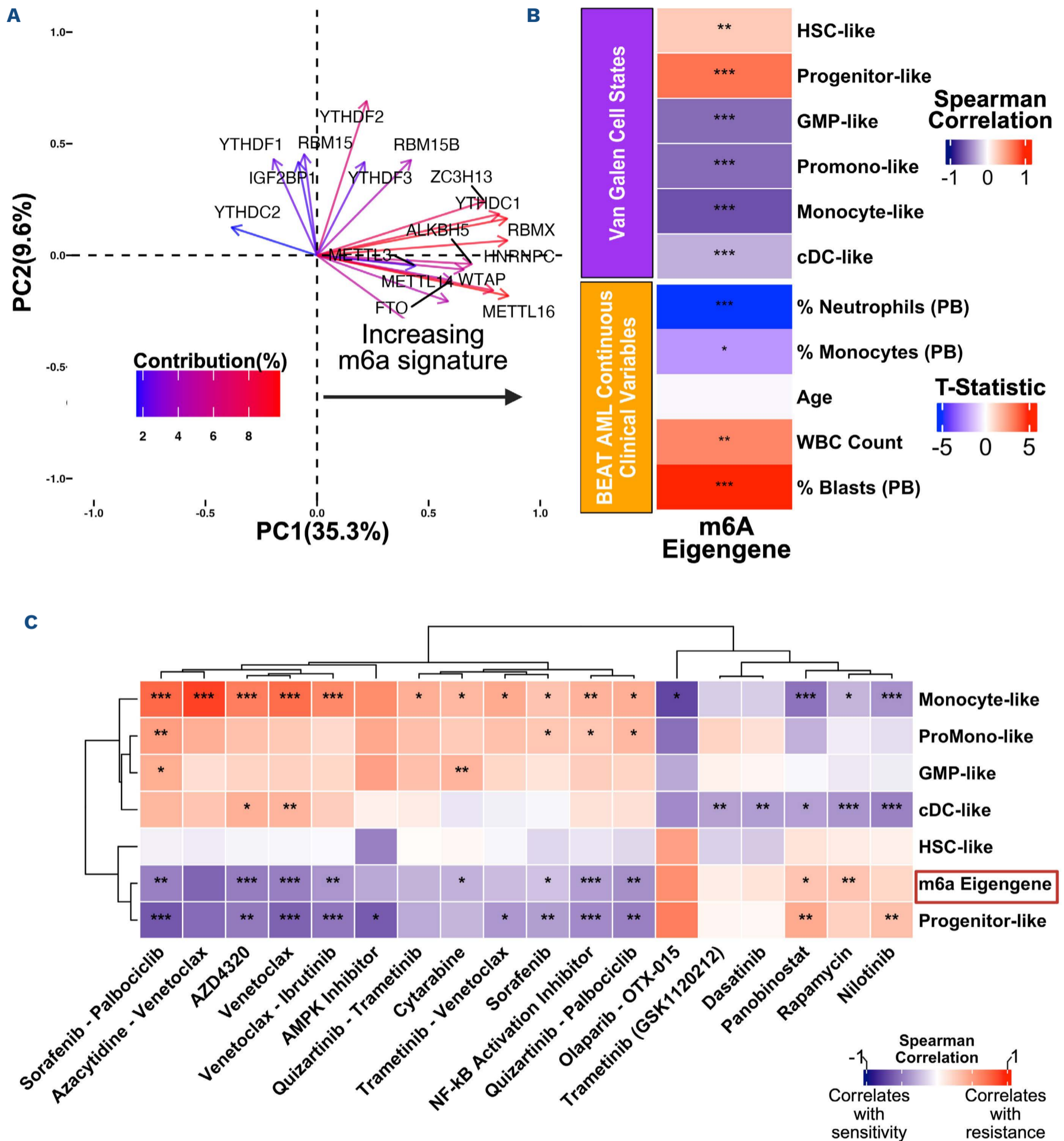


Figure 5. m6A pathway activity from the BEAT AML dataset is associated with acute myeloid leukemia differentiation and drug resistance. (A) Biplot showing member contribution in the principal component analysis of protein levels of m6A pathway genes from the BEAT AML dataset to generate an m6A eigengene-like signature (* $P < 0.05$, ** $P < 0.01$, *** $P < 0.001$). (B) Correlation of the m6A PC1 with cell state scores and linear regression against clinical differentiation markers, showing negative associations with more differentiated states. (C) Drug response correlations for the m6A PC1, indicating resistance to AZD4320 and venetoclax (* $FDR < 0.05$, ** $FDR < 0.01$, *** $FDR < 0.001$). PC: principal component; HSC: hematopoietic stem cells; GMP: granulocyte-monocyte progenitor; cDC: classical dendritic cell; PB: peripheral blood; WBC: white blood cell.

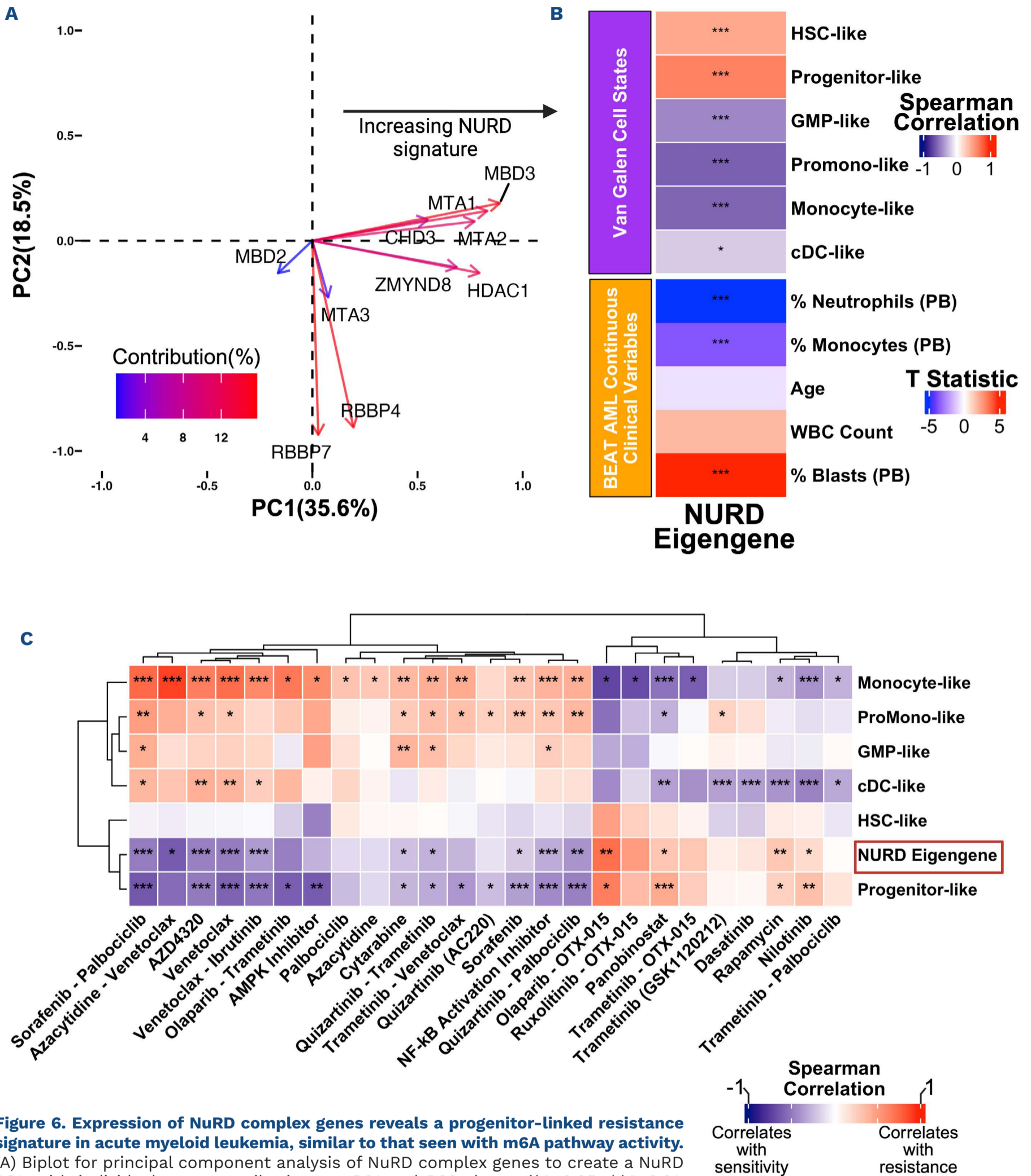


Figure 6. Expression of NuRD complex genes reveals a progenitor-linked resistance signature in acute myeloid leukemia, similar to that seen with m6A pathway activity.

(A) Biplot for principal component analysis of NuRD complex genes to create a NuRD PC1, with individual gene contributions to PC1 and PC2 shown (* $P < 0.05$, ** $P < 0.01$, *** $P < 0.001$). (B) Correlation of the NuRD PC1 with cell states and differentiation markers, also highlighting associations with more differentiated cells. (C) Drug response correlations for the NuRD PC1, showing similar resistance patterns to AZD4320 and venetoclax (* $FDR < 0.05$, ** $FDR < 0.01$, *** $FDR < 0.001$). PC: principal component; GMP: HSC: hematopoietic stem cells; GMP: granulocyte-monocyte progenitor; cDC: classical dendritic cell; PB: peripheral blood; WBC: white blood cell.

our poly-A enriched RNA-sequencing dataset, but expression of *SEMA4G* could be acting as a proxy for increased transcription of *miR-608*. Post-transcriptional control of *BCL2L1* by *miR-608* could also account for the lack of any observed correlation between *BCL2L1* expression and response to venetoclax or AZD4320 in patients' samples.

Resistance to AZD4320 in our knockout cell lines appeared to be driven by monocytic differentiation along with alterations in the expression ratios of BCL2 family members, which has previously been shown to be associated with venetoclax resistance.³⁸ *ZMYND8*-KO lines showed a reduction in BCL2 expression, especially relative to *MCL1* or *BCL2A1*, indicating a shift away from venetoclax and AZD4320 drug targets towards untargeted anti-apoptotic BCL2 members. This is consistent with the MAC-score previously shown to be predictive of clinical venetoclax response when assessing relative protein abundance of BCL2 versus *MCL1* and *BCL2L1*.³⁸ Conversely, *RBM15*-KO cells showed no shift away from BCL2 or *BCL2L1*; instead, these cells had reduced expression of the pro-apoptotic initiator *BCL2L11* (*BIM*), while increasing expression of the drug targets in a novel manner unique from prior known mechanisms of venetoclax resistance. These divergent expression changes suggest that different resistance mechanisms may necessitate distinct therapeutic strategies. For example, the setting of *ZMYND8* deficiency-related resistance would call for a combination of BCL2 inhibition with *MCL1*/*BCL2A1* targeting agents. In contrast, for *RBM15* deficiency-related cases of resistance, effective targeting strategies could include BIM stabilization or alternative apoptotic priming approaches.

Mutations and signaling activation in the RAS/MAPK pathway have been previously shown to result in venetoclax resistance *in vitro* and *in vivo*.⁴⁵ Notably, we saw no indication of activated RAS/MAPK-signaling in either knockout cell line by GSEA for signaling signatures (*Online Supplementary Figure S2A, B*), nor did we see altered response to RAF (sorafenib) or MEK (trametinib) inhibitors following knockout (*Online Supplementary Figure S1F*), demonstrating a RAS-independent mode of BCL2 inhibitor resistance. Taken together with the findings above, we conclude that monocytic differentiation with associated changes in BCL2 family expression is the primary mechanism towards resistance to venetoclax and AZD4320 in m6A- and NuRD-disrupted settings.

RBM15 is a member of the m6A RNA methylation complex, which regulates mRNA stability and translation through N6-methyladenosine (m6A) modifications. Previous studies have highlighted the role of m6A modifications in controlling myeloid differentiation and leukemogenesis. For instance, METTL3-mediated m6A methylation maintains the undifferentiated state of AML cells by promoting the translation of *MYC* and *BCL2* transcripts.²¹ Loss of *RBM15* may disrupt m6A methylation patterns, leading to altered expression of genes that promote differentiation, thereby reducing susceptibility to apoptosis induced by BCL2 inhibitors.

Similarly, *ZMYND8* is part of the NuRD chromatin remodeling complex, which influences transcriptional repression and chromatin accessibility. The NuRD complex modulates gene expression programs essential for myeloid maturation.³¹ Loss of *ZMYND8* could result in depression of differentiation-associated genes, promoting a monocytic phenotype less susceptible to BCL2 inhibition. Interestingly, *ZMYND8* has been identified as a potential therapeutic target in AML. Previous work has shown that *ZMYND8* regulates the IRF8 transcription axis and is an AML dependency, suggesting that its inhibition could impair leukemia cell proliferation.⁴⁶ However, our findings introduce a critical consideration: while targeting *ZMYND8* may reduce proliferation, it may also induce differentiation-associated resistance to current frontline BCL2 inhibitors such as venetoclax and AZD4320.

Our analyses of patient-derived AML samples revealed that lower expression levels of *RBM15* and *ZMYND8* correlated with more differentiated, monocyte-like cell states. We did not find a significant direct association between their expression levels and sensitivity to venetoclax or AZD4320, in contrast to the strong associations observed in our cell line models. This lack of correlation could be due to idiosyncratic reliance on these specific genes in the cell line models versus broader utilization of the m6A and NuRD family genes in primary patients' samples. To address this, we expanded our analysis to include the broader m6A RNA methylation and NuRD chromatin remodeling complexes. Using PCA, we discovered that the activity of these complexes is strongly negatively correlated with drug response to AZD4320 and venetoclax. The m6A and NuRD principal components negatively correlated with monocyte-like states and positively with progenitor-like states, indicating that reduced activity of these pathways is linked to increased differentiation, consistent with our observed monocytic-shift following *RBM15* or *ZMYND8* knockout. Remarkably, these principal components mapped well onto cell state scores,⁴¹ even though these signatures were unsupervised and not designed to match cell state. This underscores the significant influence of m6A RNA methylation and NuRD chromatin remodeling on AML cell differentiation and suggests that these pathways contribute to drug resistance through modulation of cellular differentiation.

Our findings reinforce the concept that the m6A and NuRD complexes are key regulators linking epigenetic and post-transcriptional modifications to AML cell differentiation and drug resistance. Targeting the m6A methylation and NuRD chromatin remodeling pathways could offer new avenues to modulate differentiation and overcome resistance to BCL2 inhibitors, potentially informing treatment plans for clinicians. Exploring combination therapies that modulate differentiation pathways or target differentiated cells while also targeting BCL2 family proteins may enhance treatment efficacy and help to circumvent resistance in AML patients.

Disclosures

JWT has received research support from Acerta, Agios, Apotose, Array, AstraZeneca, Constellation, Genentech, Gilead, Incyte, Janssen, Kronos, Meryx, Petra, Schrodinger, Seattle Genetics, Syros, Takeda, and Tolero and serves on advisory boards for Recludix Pharm, AmMax Bio, and Ellipses Pharma.

Contributions

JB-E performed investigations, was involved in software issues, validation, data analysis, and visualization, and wrote the original draft. KM and QM performed investigations and validation. SK was involved in CRISPR data analysis and methodology, and conducted investigations. DB and SKM contributed to the CRISPR screen data processing workflow methodology and tiering pipeline. TN was involved in study conceptualization, the CRISPR screen and methodology, investigations, and validation. KW-S was involved in study conceptualization, software, visualization, data analysis, and reviewing and editing the manuscript. JWT and CET were involved in study conceptualization, resources, supervision, funding acquisition, and reviewing and editing the manuscript.

Acknowledgments

We thank all patients for their generous participation. We al-

so thank the Massively Parallel Sequencing Shared Resource for Illumina sequencing support and the Flow Cytometry Core at Oregon Health & Science University.

Funding

This work was supported by the Acquired Resistance to Therapy Network (ARTNet), National Institutes of Health (NIH), National Cancer Institute (NCI) grant U54CA224019. This work was additionally supported by NCI award R01CA262758 (JWT, SEK), the Waldman Family Fund for AML Research (JWT), the George Ettelson Endowed Professorship in Acute Myeloid Leukemia Research (JWT), the Mark Foundation for Cancer Research (JWT), and the Silver Family Foundation (JWT).

Data-sharing statement

The datasets generated and analyzed during the current study are available. CRISPR screen data have been deposited in the Gene Expression Omnibus (GEO) under accession number GSE294240. All other data supporting the findings of this study are provided in the Online Supplementary Information. The code used to generate the figures and analyses is available at <https://github.com/jbrimed/m6a-nurd-aml-resistance>.

References

- Pan R, Hogdal LJ, Benito JM, et al. Selective BCL-2 inhibition by ABT-199 causes on-target cell death in acute myeloid leukemia. *Cancer Discov.* 2014;4(3):362-375.
- Youle RJ, Strasser A. The BCL-2 protein family: opposing activities that mediate cell death. *Nat Rev Mol Cell Biol.* 2008;9(1):47-59.
- Pollyea DA, Stevens BM, Jones CL, et al. Venetoclax with azacitidine disrupts energy metabolism and targets leukemia stem cells in patients with acute myeloid leukemia. *Nat Med.* 2018;24(12):1859-1866.
- DiNardo CD, Jonas BA, Pullarkat V, et al. Azacitidine and venetoclax in previously untreated acute myeloid leukemia. *N Engl J Med.* 2020;383(7):617-629.
- Carter BZ, Mak PY, Mu H, et al. Combined targeting of BCL-2 and BCR-ABL tyrosine kinase eradicates chronic myeloid leukemia stem cells. *Sci Transl Med.* 2016;8(355):355ra117.
- Chen X, Glytsou C, Zhou H, et al. Targeting mitochondrial structure sensitizes acute myeloid leukemia to venetoclax treatment. *Cancer Discov.* 2019;9(7):890-909.
- Nechiporuk T, Kurtz SE, Nikolova O, et al. The TP53 apoptotic network is a primary mediator of resistance to BCL2 inhibition in AML cells. *Cancer Discov.* 2019;9(7):910-925.
- Kuusanmäki H, Dufva O, Vähä-Koskela M, et al. Erythroid/megakaryocytic differentiation confers BCL-XL dependency and venetoclax resistance in acute myeloid leukemia. *Blood.* 2023;141(13):1610-1625.
- Pei S, Pollyea DA, Gustafson A, et al. Monocytic subclones confer resistance to venetoclax-based therapy in patients with acute myeloid leukemia. *Cancer Discov.* 2020;10(4):536-551.
- Kuusanmäki H, Leppä A-M, Pölönen P, et al. Phenotype-based drug screening reveals association between venetoclax response and differentiation stage in acute myeloid leukemia. *Haematologica.* 2020;105(3):708-720.
- Zeng AGX, Bansal S, Jin L, et al. A cellular hierarchy framework for understanding heterogeneity and predicting drug response in acute myeloid leukemia. *Nat Med.* 2022;28(6):1212-1223.
- White BS, Khan SA, Mason MJ, et al. Bayesian multi-source regression and monocyte-associated gene expression predict BCL-2 inhibitor resistance in acute myeloid leukemia. *NPJ Precis Oncol.* 2021;5(1):71.
- Zhang H, Nakauchi Y, Köhnke T, et al. Integrated analysis of patient samples identifies biomarkers for venetoclax efficacy and combination strategies in acute myeloid leukemia. *Nat Cancer.* 2020;1(8):826-839.
- Pei S, Shelton IT, Gillen AE, et al. A novel type of monocytic leukemia stem cell revealed by the clinical use of venetoclax-based therapy. *Cancer Discov.* 2023;13(9):2032-2049.
- Eide CA, Kurtz SE, Kaempf A, et al. Clinical correlates of venetoclax-based combination sensitivities to augment acute myeloid leukemia therapy. *Blood Cancer Discov.* 2023;4(6):452-467.
- Bottomly D, Long N, Schultz AR, et al. Integrative analysis of drug response and clinical outcome in acute myeloid leukemia. *Cancer Cell.* 2022;40(8):850-864.e9.
- Kurtz SE, Eide CA, Kaempf A, et al. Associating drug sensitivity with differentiation status identifies effective combinations for acute myeloid leukemia. *Blood Adv.* 2022;6(10):3062-3067.
- Majumder MM, Leppä A-M, Hellesøy M, et al. Multi-parametric

- single cell evaluation defines distinct drug responses in healthy hematologic cells that are retained in corresponding malignant cell types. *Haematologica*. 2020;105(6):1527-1538.
19. Balachander SB, Criscione SW, Byth KF, et al. AZD4320, a dual inhibitor of Bcl-2 and Bcl-xL, induces tumor regression in hematologic cancer models without dose-limiting thrombocytopenia. *Clin Cancer Res*. 2020;26(24):6535-6549.
 20. Wilson WH, O'Connor OA, Czuczman MS, et al. Navitoclax, a targeted high-affinity inhibitor of BCL-2, in lymphoid malignancies: a phase 1 dose-escalation study of safety, pharmacokinetics, pharmacodynamics, and antitumour activity. *Lancet Oncol*. 2010;11(12):1149-1159.
 21. Vu LP, Pickering BF, Cheng Y, et al. The N6-methyladenosine (m6A)-forming enzyme METTL3 controls myeloid differentiation of normal hematopoietic and leukemia cells. *Nat Med*. 2017;23(11):1369-1376.
 22. Patil DP, Chen C-K, Pickering BF, et al. m6A RNA methylation promotes XIST-mediated transcriptional repression. *Nature*. 2016;537(7620):369-373.
 23. Ma Z, Morris SW, Valentine V, et al. Fusion of two novel genes, RBM15 and MKL1, in the t(1;22)(p13;q13) of acute megakaryoblastic leukemia. *Nat Genet*. 2001;28(3):220-221.
 24. Xue Y, Wong J, Moreno GT, Young MK, Côté J, Wang W. NURD, a novel complex with both ATP-dependent chromatin-remodeling and histone deacetylase activities. *Mol Cell*. 1998;2(6):851-861.
 25. Li N, Li Y, Lv J, et al. ZMYND8 reads the dual histone mark H3K4me1-H3K14ac to antagonize the expression of metastasis-linked genes. *Mol Cell*. 2016;63(3):470-484.
 26. Najm FJ, DeWeirdt P, Moore MM, et al. Chromatin complex dependencies reveal targeting opportunities in leukemia. *Nat Commun*. 2023;14(1):448.
 27. Yoshida T, Hazan I, Zhang J, et al. The role of the chromatin remodeler Mi-2 β in hematopoietic stem cell self-renewal and multilineage differentiation. *Genes Dev*. 2008;22(9):1174-1189.
 28. DepMap 24Q4 Public. <https://doi.org/10.25452/figshare.plus.27993248.v1>
 29. Weng H, Huang H, Wu H, et al. METTL14 inhibits hematopoietic stem/progenitor differentiation and promotes leukemogenesis via mRNA m6A modification. *Cell Stem Cell*. 2018;22(2):191-205.e9.
 30. Ma X, Renda MJ, Wang L, et al. Rbm15 modulates Notch-induced transcriptional activation and affects myeloid differentiation. *Mol Cell Biol*. 2007;27(8):3056-3064.
 31. Miccio A, Wang Y, Hong W, et al. NuRD mediates activating and repressive functions of GATA-1 and FOG-1 during blood development. *EMBO J*. 2010;29(2):442-456.
 32. Tzelepis K, Koike-Yusa H, De Braekeleer E, et al. A CRISPR dropout screen identifies genetic vulnerabilities and therapeutic targets in acute myeloid leukemia. *Cell Rep*. 2016;17(4):1193-1205.
 33. Martin M. Cutadapt removes adapter sequences from high-throughput sequencing reads. *EMBnet.journal*. 2011;17(1):10-12.
 34. Langmead B, Salzberg SL. Fast gapped-read alignment with Bowtie 2. *Nat Methods*. 2012;9(4):357-359.
 35. Barnett DW, Garrison EK, Quinlan AR, Strömberg MP, Marth GT. BamTools: a C++ API and toolkit for analyzing and managing BAM files. *Bioinformatics*. 2011;27(12):1691-1692.
 36. Robinson MD, Oshlack A. A scaling normalization method for differential expression analysis of RNA-seq data. *Genome Biol*. 2010;11(3):R25.
 37. Punnoose EA, Levenson JD, Peale F, et al. Expression profile of BCL-2, BCL-XL, and MCL-1 predicts pharmacological response to the BCL-2 selective antagonist venetoclax in multiple myeloma models. *Mol Cancer Ther*. 2016;15(5):1132-1144.
 38. Waclawiczek A, Leppä A-M, Renders S, et al. Combinatorial BCL2 family expression in acute myeloid leukemia stem cells predicts clinical response to azacitidine/venetoclax. *Cancer Discov*. 2023;13(6):1408-1427.
 39. Touzeau C, Dousset C, Le Gouill S, et al. The Bcl-2 specific BH3 mimetic ABT-199: a promising targeted therapy for t(11;14) multiple myeloma. *Leukemia*. 2014;28(1):210-212.
 40. Franzén O, Gan L-M, Björkegren JLM. PanglaoDB: a web server for exploration of mouse and human single-cell RNA sequencing data. *Database (Oxford)*. 2019;2019:baz046.
 41. van Galen P, Hovestadt V, Wadsworth II MH, et al. Single-cell RNA-seq reveals AML hierarchies relevant to disease progression and immunity. *Cell*. 2019;176(6):1265-1281.e24.
 42. Tyner JW, Tognon CE, Bottomly D, et al. Functional genomic landscape of acute myeloid leukaemia. *Nature*. 2018;562(7728):526-531.
 43. Colletti GA, Miedel MT, Quinn J, Andharia N, Weisz OA, Kiselyov K. Loss of lysosomal ion channel transient receptor potential channel mucolipin-1 (TRPML1) leads to cathepsin B-dependent apoptosis. *J Biol Chem*. 2012;287(11):8082-8091.
 44. Zhang X, Fang J, Chen S, Wang W, Meng S, Liu B. Nonconserved miR-608 suppresses prostate cancer progression through RAC2/PAK4/LIMK1 and BCL2L1/caspase-3 pathways by targeting the 3'-UTRs of RAC2/BCL2L1 and the coding region of PAK4. *Cancer Med*. 2019;8(12):5716-5734.
 45. Zhang Q, Riley-Gillis B, Han L, et al. Activation of RAS/MAPK pathway confers MCL-1 mediated acquired resistance to BCL-2 inhibitor venetoclax in acute myeloid leukemia. *Signal Transduct Target Ther*. 2022;7(1):51.
 46. Cao Z, Budinich KA, Huang H, et al. ZMYND8-regulated IRF8 transcription axis is an acute myeloid leukemia dependency. *Mol Cell*. 2021;81(17):3604-3622.e10.